Univerzita Komenského v Bratislave

Fakulta matematiky, fyziky a informatiky

Jakub Zeman

Autoreferát dizertačnej práce

Development and utilization of IBA techniques for material analysis

na získanie akademického titulu philosophiae doctor

v odbore doktorandského štúdia:

Jadrová a subjadrová fyzika

Miesto a dátum:

Bratislava, apríl 2017

Dizertačná práca bola vypracovaná
v dennej forme doktorandského štúdia

na Katedre jadrovej fyziky a biofyziky, Fakulty matematiky, fyziky a informatiky, Univerzity Komenského v Bratislave

Predkladateľ: **Jakub Zeman**
Fakulta matematiky, fyziky a informatiky
Mlynská Dolina
842 48 Bratislava

Školiteľ: **prof. RNDr. Pavel Povinec, DrSc.**

Oponenti: **prof. Ing. Vladimír Nečas, PhD.**
Fakulta elektrotechniky a informatiky STU v Bratislave
Ilkovičova 3, 812 19 Bratislava

Ing. Ján Kliman, DrSc.
Fyzikálny ústav SAV
Slovenská akadémia vied
Dúbravská cesta 9, 845 11 Bratislava

Dr. Alfred Priller, PhD.
University of Vienna
Faculty of Physics
Isotope Research and Nuclear Physics
Waehringer Strasse 17, 1090 Vienna, AUSTRIA

Obhajoba dizertačnej práce sa koná ..... o ..... hod
pred komisiou pre obhajobu dizertačnej práce v odbore doktorandského štúdia vymenovanou predsedom odborovej komisie .....
(uviesť dátum vymenovania)

odbor: Jadrová a subjadrová fyzika, študijný program: 4.1.5. Jadrová a subjadrová fyzika

na Katedre jadrovej fyziky a biofyziky, Fakulty matematiky, fyziky a informatiky, Univerzity Komenského v Bratislave, Mlynská dolina, 842 48 Bratislava

Predseda odborovej komisie:

Prof. RNDr. Jozef Masarik, DrSc.
FMFI UK
Mlynská dolina
84248 Bratislava

.....
(meno a priezvisko s uvedením titulov a hodností
a presná adresa jeho zamestnávateľa)

Contents

Introduction

In November 2015 a new laboratory for nuclear and environmental research and for development of nuclear technologies was established at the Department of Nuclear Physics and Biophysics at the Faculty of Mathematics, Physics and Informatics of the Comenius University in Bratislava. This laboratory was given a name CENTA (Centre for Nuclear and Accelerator Technologies). The facility is equipped with a system that is capable of various ions production and their further application and analysis. The main device in the laboratory is an electrostatic linear tandem accelerator, which is designed for obtaining of ion beams with acquired attributes (energy, intensity etc.). The main scientific purpose of the laboratory is the gradual implementation and consecutive utilization of ion beam techniques and methods primary in nuclear and environmental sciences. The idea is to extend the area of research on new material development and surface treatment of materials using ion beams.

The basic equipment of the laboratory consists of two ion sources – Alphatross for gaseous targets and MC-SNICS for solid targets; 3 MV electrostatic linear tandem accelerator Pelletron; electrostatic analyzer; two bending magnets and a magnetic quadrupole triplet.
The techniques that are being developed in the laboratory can be divided in 3 groups:

1.) IBA – Ion Beam Analysis, techniques for material and sample analysis.
2.) AMS – Accelerator Mass Spectrometry, specifying of isotope content in various samples.
3.) IBM – Ion Beam Modification, techniques for material surface treatment, material aging in high ion flows etc.

The thesis presents developments of IBA techniques and their utilization in material research. Basic and crucial characteristics of IBA techniques are described. PIXE analyzes have begun after successful installation of PIXE/PIGE chamber in September 2015. The journey to presented achieved results contains of calibration and optimization of whole acceleration and detection system. Experimental setup installed in the CENTA laboratory is described and main ion optics devices highlighted. Results of Pelletron transmission efficiency measurements, SIMION simulations of helium beam profile at the end of beam line, calibration and optimization of PIXE/PIGE chamber are presented. Results of performed PIXE analyzes are concerned as well.

Goals of the dissertation thesis

The goals of the thesis may be summarized as follows:

(i) Ion beam trajectory simulations using SIMION software.

(ii) Ion source optimization for proton and helium beams production using the ALPHATROSS ion source, and for beryllium and carbon beams using the MC-SNICS ions source.

(iii) Investigations of tandem accelerator transmissions for protons, helium, beryllium and carbon ions.

(iv) Optimization of the analyzing beam line.

(v) Development of IBA techniques (PIXE, PIGE) for elemental analyzes of materials.

(vi) Calibration methods and interpretation of acquired results.

Achieved results

Results of system calibration, optimization and analyzes can be divided into 4 categories:

A) Pelletron transmission efficiency measurements

B) Ion beam profile simulations at the end of the beam line

C) PIXE analysis methods in the CENTA laboratory

D) Determination of H values for PIXE analyzes and analyzes themselves

A) Pelletron transmission efficiency measurements

The quality of stripping process is defined by transmission efficiency. In literature it is possible to find different terms such as stripping efficiency or stripping yield [Steier, 2000], or charge state fraction [Winkler, 2015], or transmission efficiency [Maxeiner, 2015], but all of them describe the same quantity. Transmission efficiency is used for description of stripping process effectiveness for different ions and different charge states of a certain ion. Negative ions enter stripping channel, i.e., volume of beam line which contains stripper gas. Via interactions with gas molecules, electrons are being stripped from negative ions so the ions become positive. Depending on the ion mass, the stripper gas pressure and the energy of ions, various final charge states of positive ions are being accelerated in the second phase of the tandem acceleration process. Consequently, ions gain various amount of acceleration so they are leaving the Pelletron at different energies. Knowledge of the stripping process quality is very important for analysis of ions and for further applications.

The transmission efficiency was determined for ^{1}H, ^{4}He, ^{9}Be and ^{12}C ion beams. Protons and helium ions were produced in Alphatross, beryllium and carbon ions were produced in MC-SNICS. The ions' injected energy from the sources was set to 52 keV for ^{1}H and ^{4}He and 61 keV for ^{9}Be and ^{12}C. Pelletron is designed for maximal terminal voltage of 3MV. Most of the measurements were done for 6 values of terminal voltage: 1.5 MV, 1.8 MV, 2.1 MV, 2.4 MV, 2.7 MV and 3.0 MV. Results for protons and helium are shown in Fig. 1. Beryllium results are displayed in Fig. 2. Measurements and results of ^{12}C ion beam transmission efficiency can be found in [Zeman, 2016] and also some results for ^{9}Be and ^{12}C were published in [Povinec, 2016].

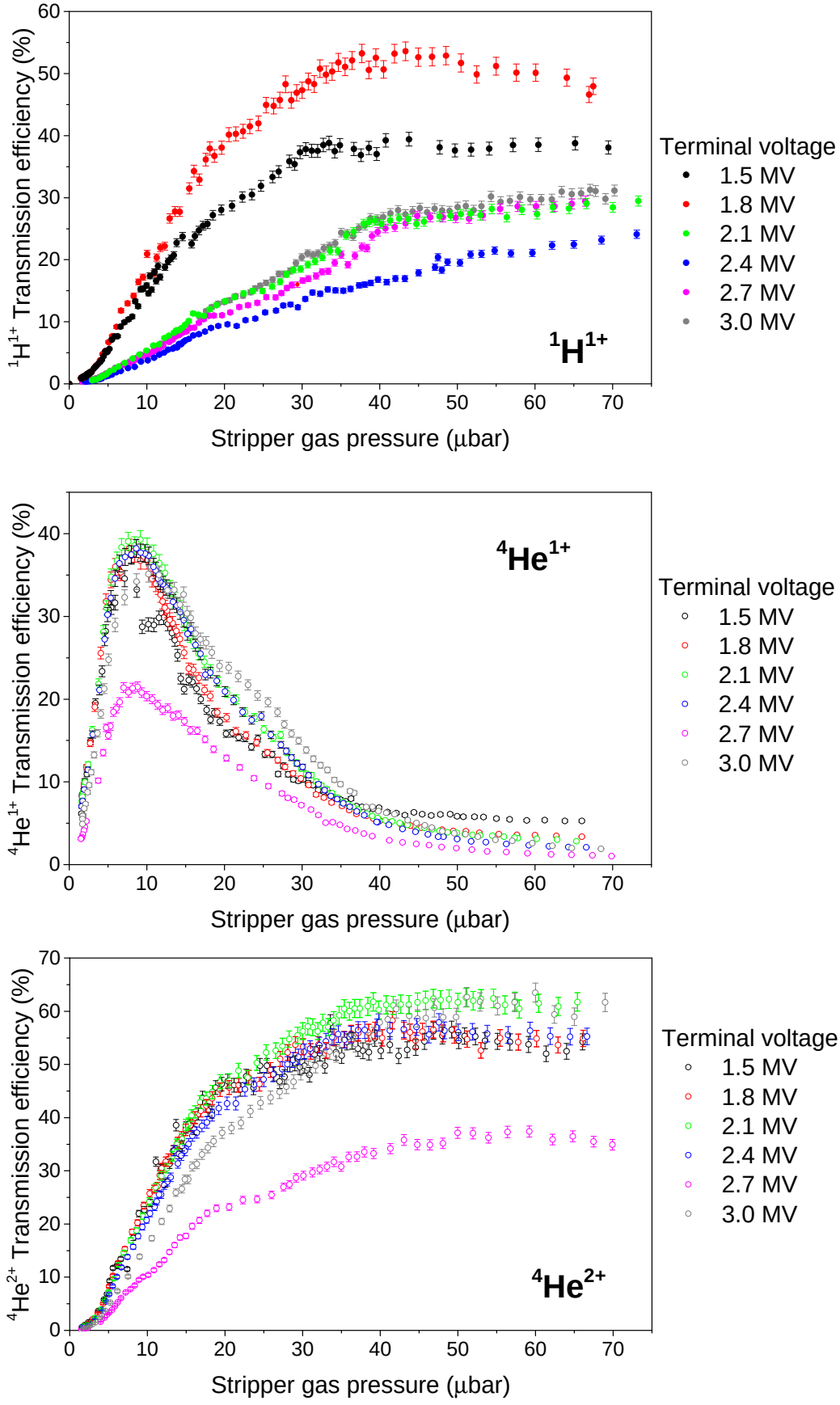

Fig. 1: Transmission efficiency of protons and helium for all measured terminal voltages

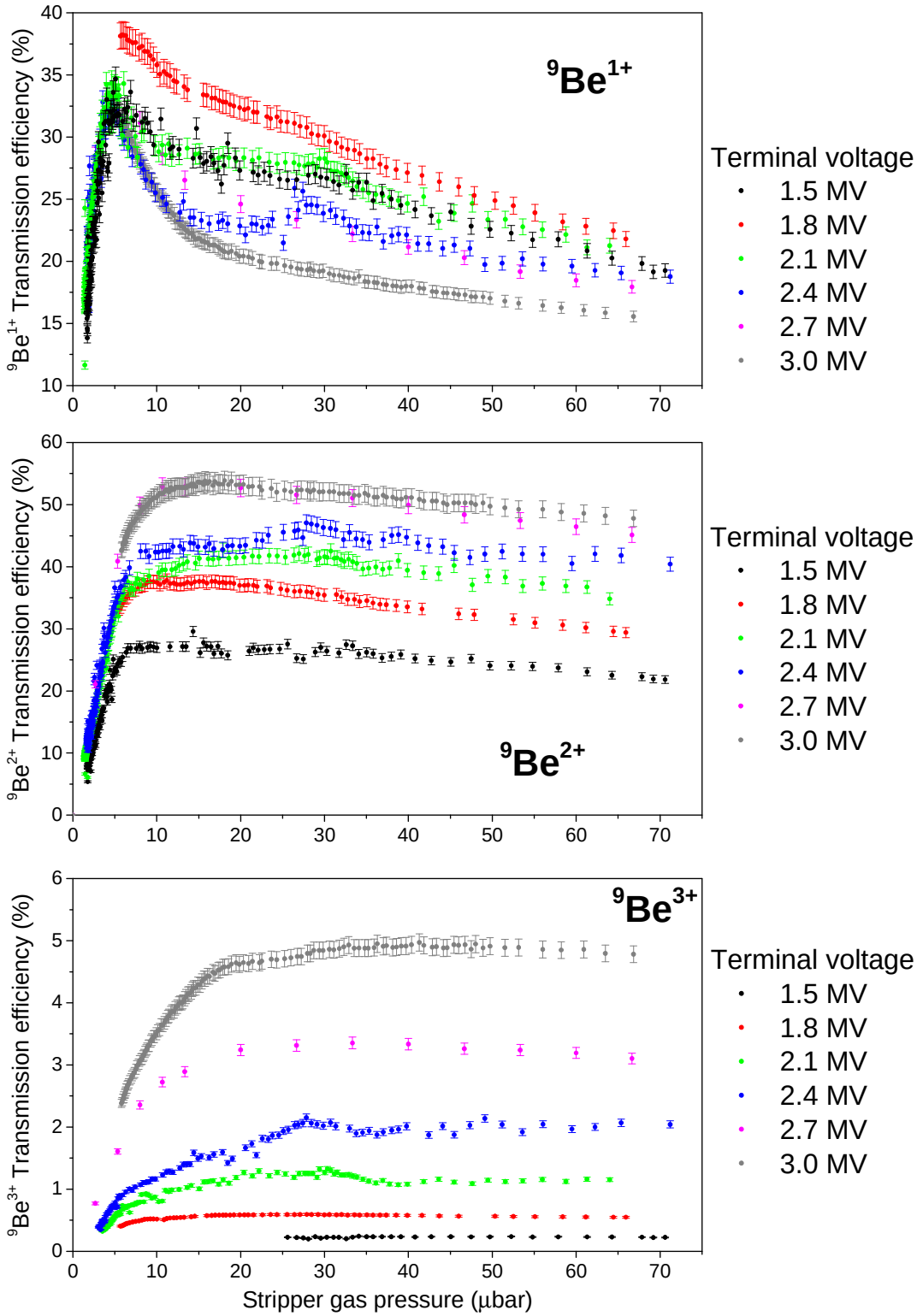

Fig. 2: Beryllium transmission efficiency values for all monitored terminal voltages. The stripper gas pressure scale is the same in all graphs. The transmission efficiency scales are different for individual charge states.

Maximal values of the transmission efficiencies for ^{1}H, ^{4}He, ^{9}Be and ^{12}C ions are listed in Table 1. Some maximal values were observed for the same charge state at different terminal voltages. These values are recorded both.

Ion	Charge state	Terminal voltage (MV)	Strip. gas pressure (μbar)	Transmission efficiency (%)
^{1}H	1+	1.8	43	53.6 ± 1.5
^{4}He	1+	2.1	9	39.3 ± 1.1
	2+	2.1	51	62.6 ± 1.8
	2+	3.0	60	63.5 ± 1.8
^{9}Be	1+	1.8	6	38.2 ± 1.1
	2+	2.7	13	52.9 ± 1.4
	2+	3.0	16	53.8 ± 1.5
	3+	3.0	41	5.0 ± 0.2
^{12}C	2+	1.8	11	42.3 ± 1.1
	3+	2.7	27	47.7 ± 1.2
	4+	2.7	40	20.5 ± 0.9

Table 1: Maximal measured values of transmission efficiency for individual ion beams. Values for smooth dependencies were taken from the highest points, but the efficiency was more-less stable at wide range of stripping gas pressure.

B) Ion beam profile simulations at the end of the beam line

Two main ion optics devices installed in the CENTA laboratory at the end of current beam line are magnetic quadrupole triplet lens (QP) and switching magnet (SM). The aim of simulations was to find out how the transverse beam profile changes at the end of the beam line when passing through the QP and SM. For this purpose SIMION software was used. This program enables user to create a models for ion optics devices for 2D symmetric and/or 3D asymmetric electrostatic and magnetic fields. 3D CAD models were "installed" into SIMION's workbench environment in proper geometry (Fig. 3). The SM's magnetic flux density (B) was set in simulations to bend the trajectory into 45° analyzing beam line. Next, in the distance corresponding to the end of this beam line, a target foil was placed to obtain information about transversal beam profile after ions incidence.

3.052 MeV $^{4}He^{2+}$ ion beam was monitored. The initial transversal beam profile was set to symmetrical circular with Gaussian distribution around the center (position 0,0). The FWHM was set to 5 mm. This value was selected because this is the assumption for transversal profile of beam exiting the Pelletron and entering the focusing beam line. Transversal profile of $^{4}He^{2+}$ ion beam is shown in Fig. 4. This beam was passing through QP and SM in simulations.

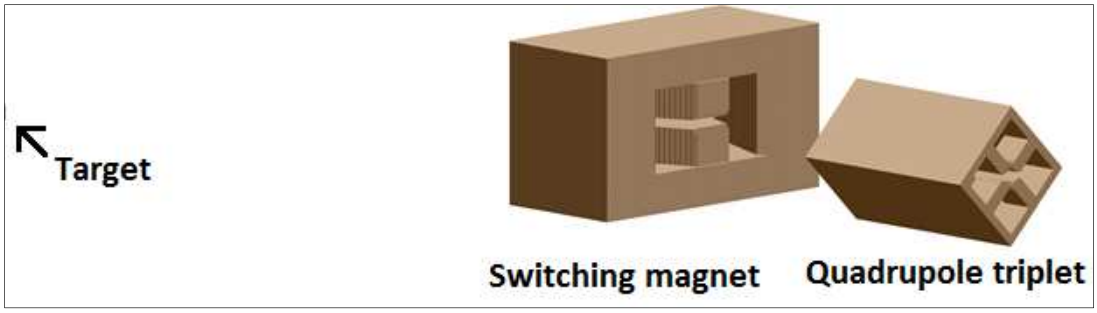

Fig. 3: SIMION workbench layout of simulations for SM and QP – side view with beam incoming from the right into the QP. The target represents a small plane which was used as target foil where the beam profile was monitored. The target was placed into 2085 mm distance from the exit edge of SM what corresponded to the real target distance in 45° analyzing beam line.

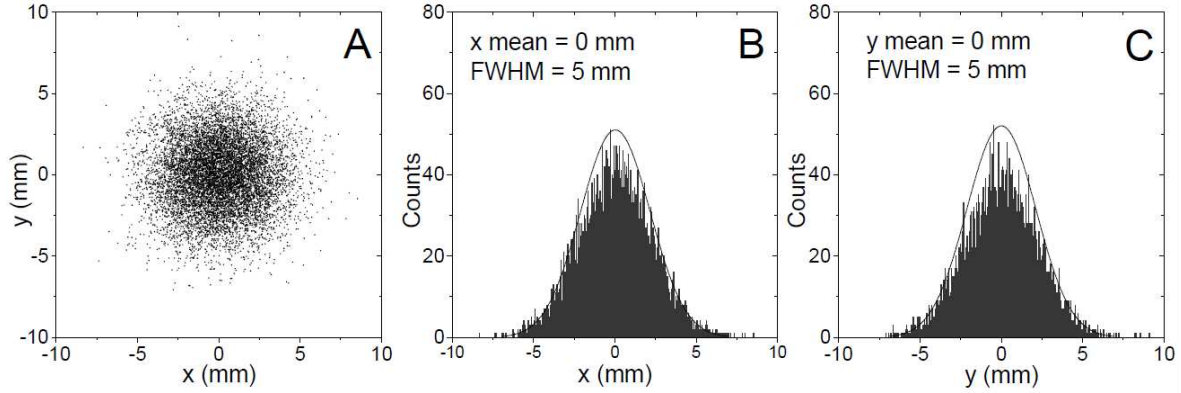

Fig. 4: Transversal profile of $^{4}He^{2+}$ ion beam used in simulations (A), horizontal dimension (B) and vertical dimension (C). Ions in the beam were Gaussian distributed around the center – position (0,0). The FWHM was 5 mm. The amount of ions was 10 000.

Various settings of QP were tested and finally, an appropriate setting of QP's magnetic field flux density was found. Satisfying results are shown in the Fig. 5. The original beam with 5 mm diameter was focused into smaller diameter of ~ 1.4 mm. Currently (April 2017), these settings are the best reached. With further adjusting of QP in simulations larger beam diameters were observed.

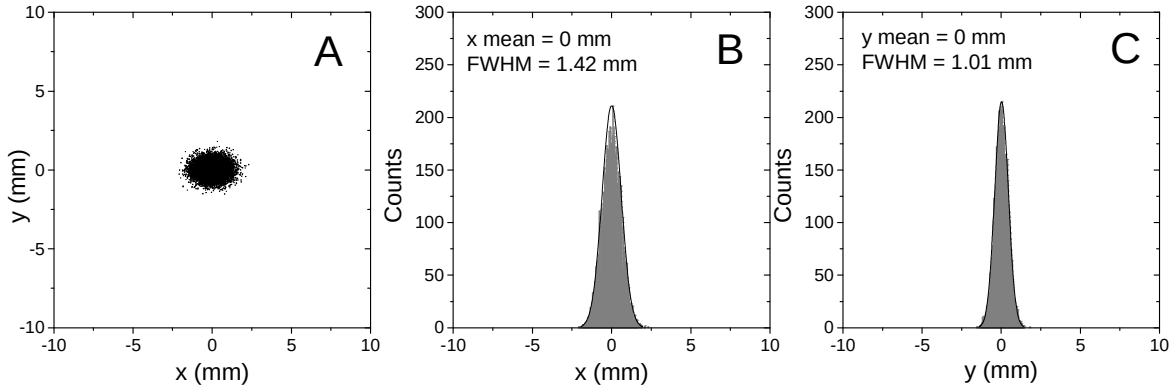

Fig. 5: Transversal profile of $^{4}He^{2+}$ ion beam (A), horizontal (B) and vertical (C) dimension.

C) Development of the PIXE analysis methods in the CENTA laboratory

A PIXE chamber was installed in the laboratory (September 2015) thanks to the IAEA funding. Details about the chamber can be found in [Zeman, 2016B]. The chamber is equipped with a sample holder capable of mounting four thick samples of about 2×2 cm dimension. The holder can be rotated around its vertical axis, so the angle how the incident beam should hit the sample can be fixed. For the charge collection, digital current integrator (Ortec Model 439) is used. A schematic top view of the chamber is shown in Fig. 6 (left part). The chamber itself is formed by a 6-way cross, where BEGe detector (CANBERRA) and a sample holder (NEC) are placed (detector endcap can be seen in Fig. 6 on the right photography). The detector has a carbon window (0.6 mm thickness). The detector is used for detection of emitted X-rays covering the energy range from 3 keV to 3 MeV, with energy resolution of 390 eV for 5.9 keV (^{55}Fe) and 1.8 keV for 1332 keV (^{60}Co). Necessary vacuum components (gate valves, turbo pump…) are installed as well.

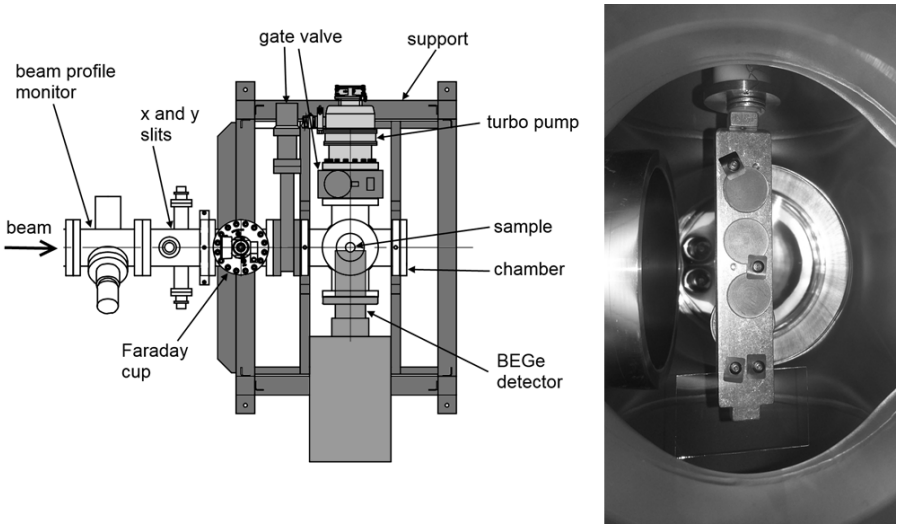

Fig. 6: Top view of the PIXE/PIGE chamber (left), and mounted pressed metallic powder samples inside the chamber (right) [Zeman, 2016B].

The original installation of detector was changed later in summer 2016. The detector was shifted outside from the chamber using additional pipe. The purpose was to improve the detector background. At PIXE measurements, depending on the parameters of used beam (ion type, energy, intensity), and also on the target angle to the incident beam, various background was observed in BEGe detector. The majority of this unwanted background originates from the bremsstrahlung. The idea was to reduce this effect by shifting the detector further from the interaction point. This geometry is shown in the Fig. 7.

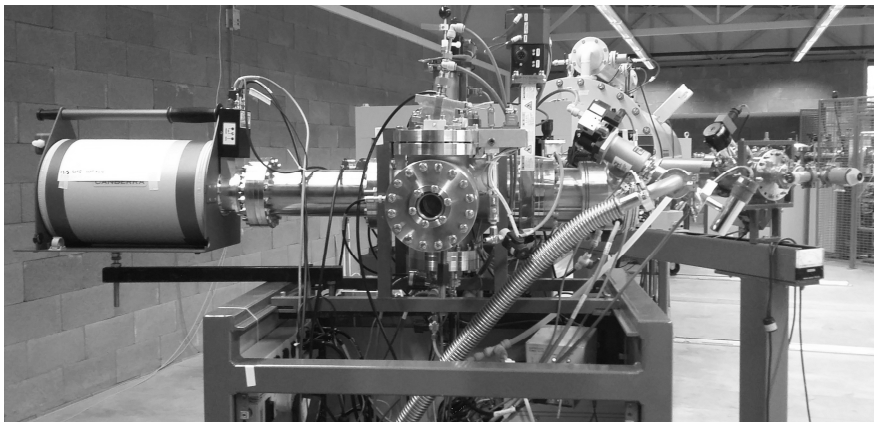

Fig. 7: BEGe detector shifted using additional pipe. The endcap distance from the center of PIXE chamber increased to 25 cm.

This shift had a positive effect on the background reduction (Fig. 8). The same beam (3 MeV protons, for the same time as after the shift) used before, created on the glass sample higher background compared to the shifted situation. The increased distance, on the other hand, resulted in detection efficiency loss. This loss is acceptable, since the reduction of background brought better resolution for low energies. In Fig. 8, the gray spectrum (corresponding to BEGe shift) exhibit better resolution, so peaks in the beginning could be resolved better.

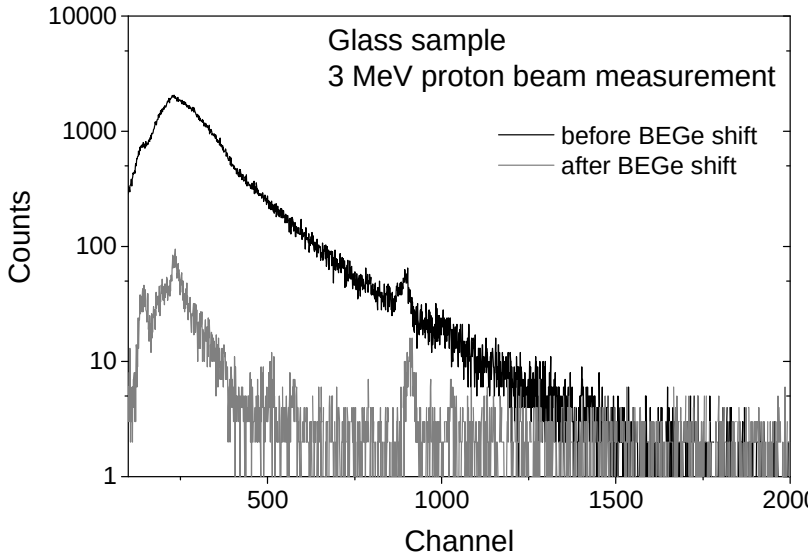

Fig. 8: Background spectra before (black) and after (gray) the BEGe detector shift.

The very important role in the PIXE measurements plays the sample holder. For analytical purposes, the total amount of ions which induce the X – ray (or gamma) emission have to be known precisely. This is obtained via the charge collection from the sample holder. The holder is electrically insulated from the chamber. A thin wire mounted to the sample holder is transferring the signal through the feedthrough on the top of the chamber. The

incident ions bring a positive charge, which is collected by this wire. The signal is processed by Ortec digital current integrator with inaccuracy 1.81 % for low beam current (1 –2 nA). Depending on the charge state of incident ions, their amount can be calculated.

In the CENTA laboratory, after the PIXE/PIGE beam line installation, the technique development proceeded in 3 steps:

1.) BEGe detector calibration and efficiency determination
2.) Additional adjustment for proper charge collection
3.) PIXE spectra interpretation

BEGe detector calibration and efficiency determination

BEGe detector calibration was performed using calibrated X – ray variable sources and gamma ray sources. The calibration was performed for energy range up to ~ 60 keV. The range was selected in order to observe X – ray lines from the lower energy spectrum. In PIXE measurements, only X – ray lines up to 30 keV have been observed, as is described later.

The detector efficiency was determined using point sources measurements and detector efficiency modeled using DETMC software (created by The Guelph PIXE Group, Department of Physics, University of Guelph, Canada). This software was supplied with the GUPIXWIN software, which was a part of PIXE/PIGE beam line package. The DETMC program is a Monte Carlo tool for calculating Si(Li), SDD, and Ge detector efficiency.

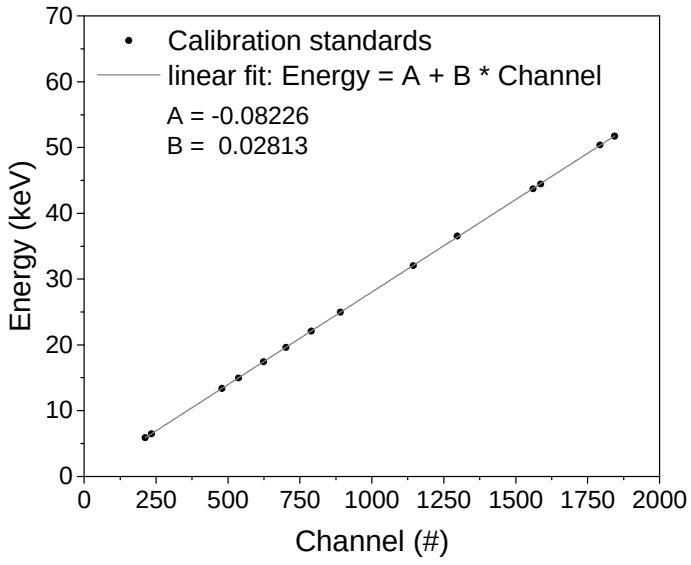

Fig. 9: BEGe detector energy calibration for 0 – 60 keV range

Calibrated point sources (with known activities) were placed at 25 cm distance from the detector endcap. Each point source was measured individually and spectra were analyzed in

order to determine peak areas and then calculate the absolute efficiency. Unfortunately, the sources' energies that were at disposition started at ~ 30 keV, thus the efficiency for lower energies can be taken only from the model. At energy 11.1 keV the efficiency drops because of germanium K-absorption edge. Energy of photon in close proximity to this value is more likely to be absorbed.

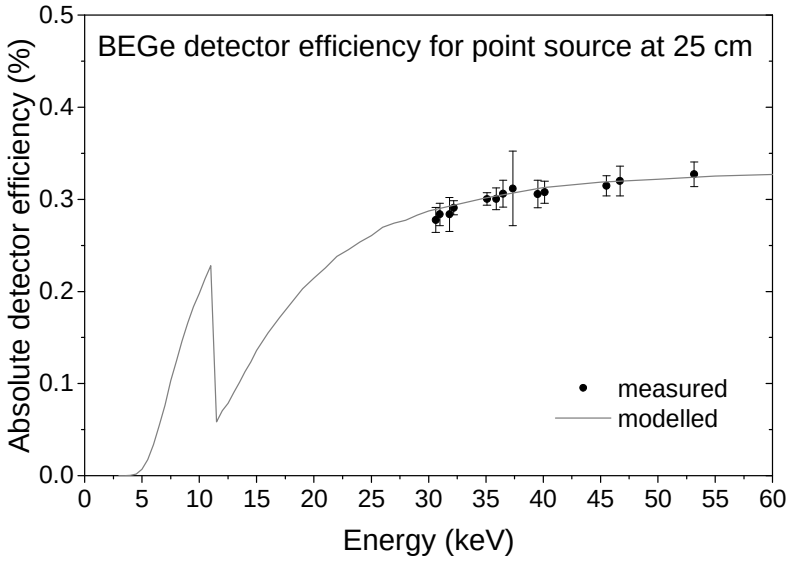

Fig. 10: BEGe detector efficiency for point source at 25 cm distance. The gray line represents the modeled values (DETMC program). The black dots are calculated efficiencies from measurements. Areas of some peaks used for evaluation were small, therefore some values exhibit higher uncertainties (e.g. 37.35 keV).

Adjustments for proper ion charge collection

Information about accurate amount of particles which induce the X–ray emission have to be known precisely in order to perform quantitative analysis. Incident ions interact with the sample which is mounted on a sample holder inside the PIXE chamber. The sample holder is conductively connected via thin spring wire with digital current integrator (DCI). The DCI is connected with the software which collects the data during the measurements (spectra, time period, settings of MCA). The total amount of ions is important in element concentration calculations.

For quantitative analyzes, the charge collection had to be done precisely. The original setup for sample holder inside the chamber (Fig. 6, the right photography) did not include system for secondary emitted electrons suppression. This phenomenon plays important (and negative) role in the charge collection process. Impact of positive ions causes emission of secondary electrons. In this process, as the result of electrostatic induction, the irradiated material is charged positively. This excess of positive charge is collected by the DCI together

with the positive charge brought by the incident ion beam. Therefore, after conversion of collected charge, it seems that the beam is formed by more particles than it really is. Consequently, misleading results are obtained from sample composition analysis. The negative effect of secondary electrons emission can be suppressed using more methods. In the CENTA laboratory, option for secondary electrons suppression electrode was chosen.

Fig. 11: Front and top view of the suppressor electrode as it was installed into the chamber

The design of this suppressor electrode is based on SIMION simulations. More combinations of rod thickness, diameter of the rings and vertical distance of the 2 rings were simulated. Finally, 5 mm thick rod, 80 mm diameter of rings and their vertical distance of 30 mm came out as the most suitable solution for the chamber conditions. The SIMION model and results of simulations are shown in the Figure 12.

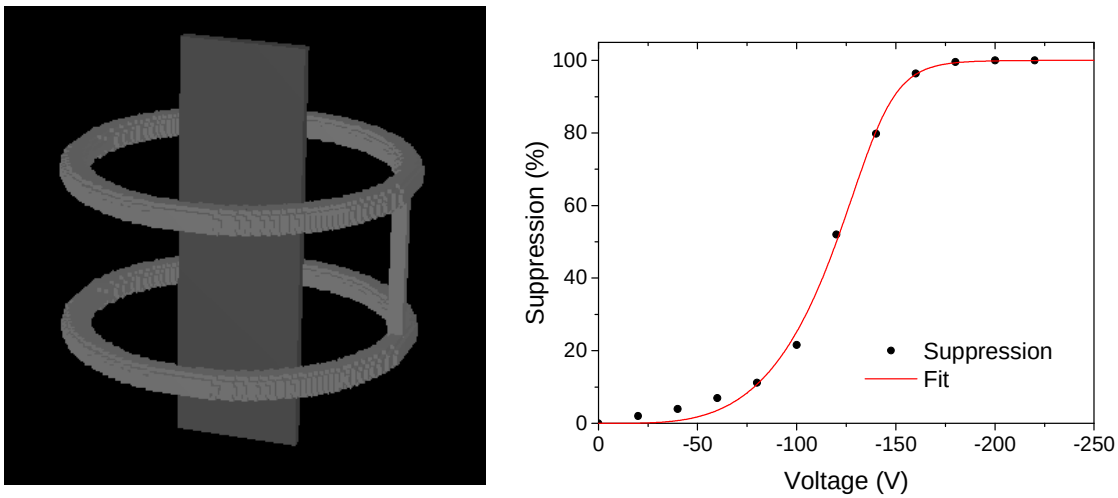

Fig. 12: SIMION model of secondary electrons suppression electrode. The model in 3D SIMION view (left) and result of simulations for electrons suppression depending on the voltage of the electrode (right). The suppression was calculated as ratio of difference between amount of created electrons and escaped electrons to amount of created electrons.

PIXE spectra interpretation and concentration calculations

In the CENTA laboratory the PIXE measurements are being performed using proton or helium beam. Energy of protons is chosen as 3.052 MeV (TV = 1.5 MV, 1+ charge state) and energy of helium 4.552 MeV (TV = 1.5 MV, 2+ charge state).

X – Rays are detected by BEGe detector and the signals are processed through preamplifier into MCA and software which collects the data. Measured spectra are analyzed using software GUPIXWIN, which was developed in University of Guelph, Canada [Maxwell, 1989], [Maxwell, 1995], [Campbell, 2000], [Campbell, 2010]. GUPIXWIN is a program for the non-linear least-squares fitting of PIXE spectra and the subsequent derivation of element concentrations from the areas of X-ray peaks in the spectrum. The output from the program can be seen in the Fig. 13 (exemplary figure).

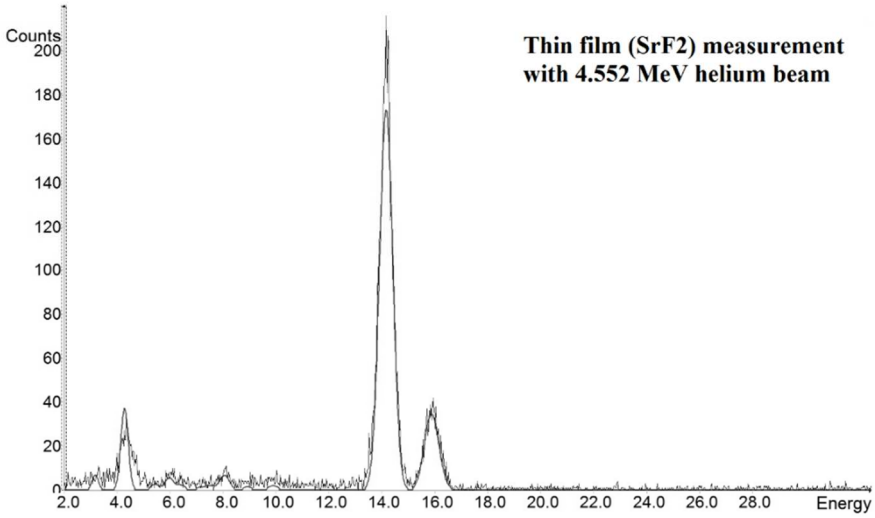

Fig. 13: GUPIXWIN fit of thin film (SrF_2) measured spectrum

The GUPIXWIN fit the spectrum considering many factors. The database includes: X-ray energies and emission rates, element densities and atomic weights, ion induced X-ray production cross-sections, proton stopping powers, photoelectric cross-sections and X-ray mass attenuation coefficients. Within the calculations, GUPIXWIN computes also corrections for escape and summation peaks.

Peak areas could be converted to element concentrations in absolute way, i.e., without standards, if the aspects of the analyzing system (solid angle, detector thickness, beam proportions, etc.) are given into GUPIXWIN. That is a "fundamental parameters" approach. Alternatively all analyses could be conducted relative to single-element standards or to

standard matrices containing various trace elements. The X-ray intensity or yield (principal X-ray line), *Y (Z,M)* for an element *Z* in a matrix *M* can be written:

$$Y\ (Z,M) = Y_{1t}\ (Z,M) * \ C_Z * Q * f_q * \ \Omega * \varepsilon * T \qquad (1)$$

where:

Y_{1t} is the theoretical (from GUPIXWIN database) intensity or yield per micro- Coulomb of charge per unit concentration per steradian;

C_z is the actual concentration of element *Z* in matrix M;

Q is the measured beam charge or quantity proportional thereto; if the latter, then f_q converts the *Q* to micro- Coulombs; if the former then f_q is 1.0 assuming proper electron suppression at the target;

Ω is the detector front face solid angle in steradians;

ε is the intrinsic efficiency of the BEGe detector;

T is the transmission through any filters or absorbers between target and detector.

The equation (1) includes multiple possible factors which influence the final element's concentration. In the CENTA laboratory, no filters are used between the sample holder and detector, thus *T* equals to 1.0. Parameters f_q and Ω can be combined into an instrumental constant *H*, which characterizes the PIXE detection system. The approach taken in GUPIXWIN employs the physics database together with a single quantity of H value. Depending on the system characterization this H value is a constant or it is function of X-ray energy. Implementing these facts, the element concentration using the equation (1) can be calculated as follows:

$$C_Z = \frac{Y\ (Z,M)}{Y_{1t}\ (Z,M)\ * \ H * Q * \ \varepsilon} \qquad (2)$$

Measured X-ray yield is converted to concentration for all elements fitted. The detector efficiency was determined in section before. In the laboratory, both thin and thick samples are being analyzed. Thin samples are considered as samples with thickness insufficient to stop the beam completely. Incident particles (in our case protons or helium ions) can penetrate through the sample. These ions have to be collected as well, so a Faraday cup was placed at the end of the beam line. For thin samples, this Faraday cup's and sample holder's charge signals were collected by the current integrator. Thickness of thick samples is sufficient to stop the beam, thus no ions penetrate through these samples and the whole charge is collected from the sample holder.

D) Determination of H values and PIXE analyzes

The H values for thin and thick samples were determined from measurements of thin films supplied by MICROMATTER™ Company (Table 2) and pressed powder samples prepared in our laboratory (Table 3). Measurements were performed under same conditions. The geometry setup scheme for the measurements is displayed in Fig. 14. The figure displays a top view of the chamber with sample holder, beam direction and BEGe detector position. The measurements were performed using the 3.052 MeV proton beam, and later using 4.552 MeV $^{4}He^{2+}$ ion beam.

film	Fe	Cu	Ga	Sr	Cd	Sn
Thickness ($\mu g/cm^2$)	49.8	48.8	23.4	54.9	45.3	52.4
Thickness (nm)	63.2	54.5	39.6	208	52.4	72.1

Table 2: The thickness of thin films stated by the manufacturer with 5.0 % accuracy ($\mu g/cm^2$) and calculated values in nanometers.

Powder	Fe	Cu	Zn	Ag
Weight (g)	2.07	2.08	1.35	1.52

Table 3: Weights of powders used for preparation of thick-pressed samples.

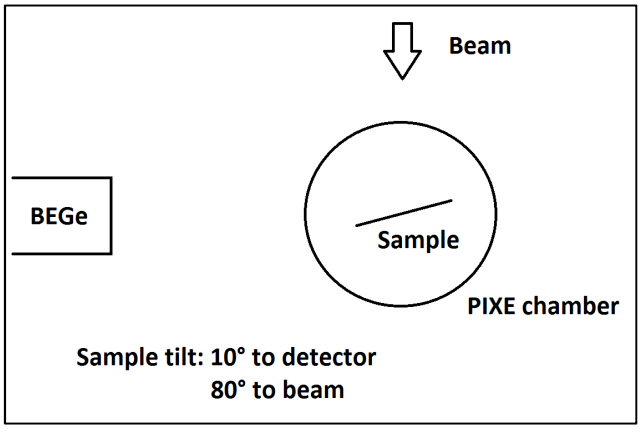

Fig. 14: A scheme of the geometry setup for thin film measurements (a top view).

Results of H value determination for thin and thick samples are shown in the Fig. 15. For proton measurements energy dependency was observed. Helium analysis exhibits more-less constant values.

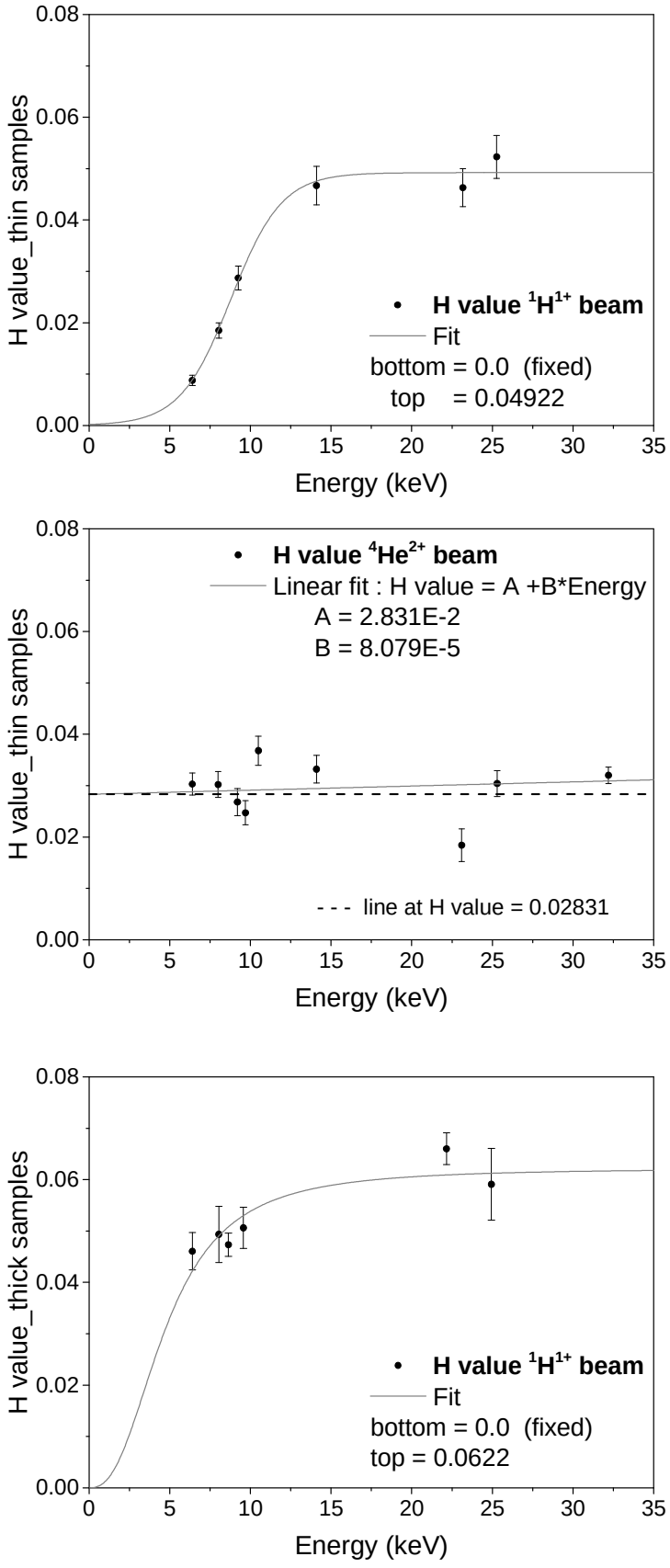

Fig. 15: Results of H value determination for thin and thick standards using 3. 052 MeV proton and 4.552 MeV $^{4}He^{2+}$ beams. Dash line at 0.02831 was added for better imagination of difference from constant value.

Concentration of iron in a rat brain sample

The CENTA laboratory has already been cooperating with several research institutions. In cooperation with Medical faculties of the Comenius University in Bratislava and Martin a rat brain slice was received to determine iron concentrations and map its distribution in the slice. The aim of this study has been to evaluate concentrations of iron in this slice on various spots. It is expected that the iron in the rat brain was produced by electromagnetic radiation similar to one generated in mobile telephones. The observed effects in the brain tissue may be due to electromagnetic radiation, which causes agglomeration of iron in the tissue. A map of iron distribution with measured concentration (which may be regarded as a simple nuclear microscopy map) should provide important information for further medical research. At present it is not well understood how this iron agglomerates in the brain tissue, but there are hypotheses that the electromagnetic radiation may cause this effect, [Terzi, 2016], [Kaplan, 2016], [Kostoff, 2013].

A thin slice of the rat brain (~5μm) was prepared for investigation. The slice was attached on a thick silicon wafer. Consequently, due to SEM measurements, a thin gold layer (~ 30 nm) was deposited on the surface of the tissue. The sample was then inserted into the PIXE chamber of the CENTA laboratory for investigations. Results of this analysis are shown in Fig. 16.

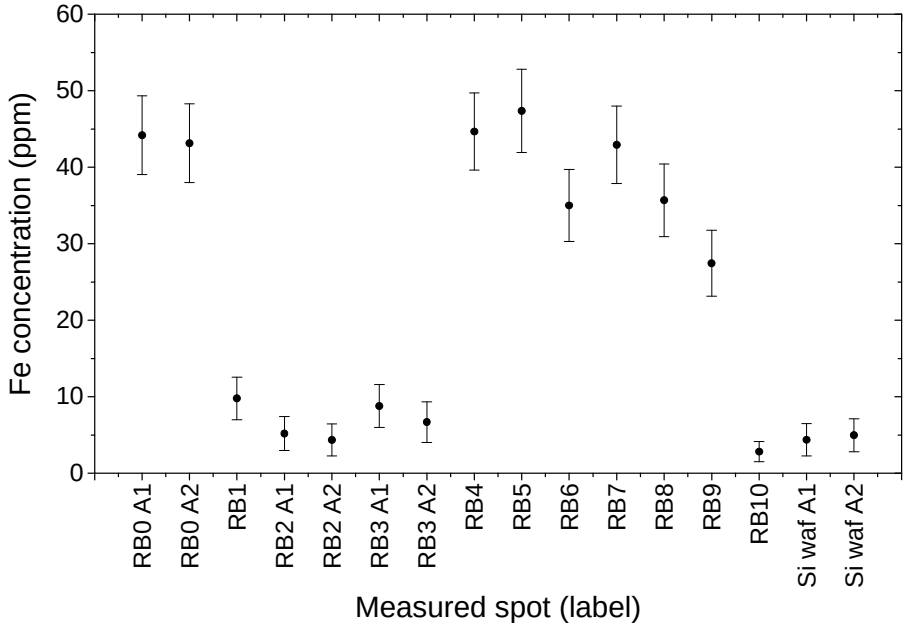

Fig. 16: Iron (Fe) concentration in rat brain sample. Measured spots on the sample are labelled as RB0 - RB10, Si wafer was measured as well. Some of the positions were analyzed twice (A1 and A2 labels). The evaluated Fe concentration for corresponding spots exhibits the same values.

Ongoing experiments

Many more samples were analyzed in the laboratory using the PIXE system. Some of the spectra were obtained before the mentioned adjustments (detector shift, electrode installation). These experiments are ongoing, and the samples will have to be measured again. Only some qualitative information about samples' composition can be retrieved from current status of these analyzes (April 2017).

PIXE analysis of meteorites

Canyon Diablo iron meteorite from Arizona was analyzed by helium PIXE beam. Iron and copper peaks are well visible (Fig. 17). New analyses are in preparation with adjusted geometry and lower beam intensity to suppress the background. Plan is to perform PIXE measurement in new condition in the chamber with proper charge collection and lower background to possibly observe more elements. Absolute concentration of individual elements will be hopefully determined after applying H values for thick samples.

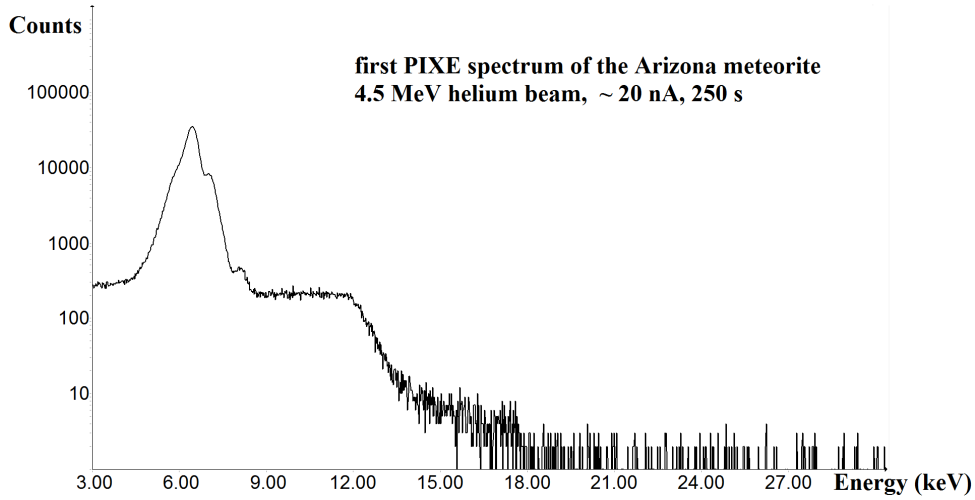

Fig. 17: First PIXE spectrum of the Canyon Diablo iron meteorite from Arizona. PIXE conditions as described in figure. The measurement was performed with high beam intensity without charge collection and before the adjustments in the PIXE chamber.

PIXE analysis of uranium in zirconium mineral

Zirconium mineral was analyzed by PIXE using the proton beam (Fig. 18). Plausible presence of more elements is described in the figure comment. This material is being analyzed in order to test whether via PIXE technique it would be possible to determine uranium content in this mineral. The idea is to detect low concentrations of this element in various geological samples as well as in reactor fuel materials (fast measurements in the case of uranium smuggling). The recent measurements showed that GUPIXWIN was able to find uranium

peak in the measured spectrum, however, it has not been possible yet to calculate its concentration because uranium L-lines lie in the region of zirconium K-line energies. It seems that a different approach should be taken in order to search for uranium in zirconium minerals, namely a use of a high resolution Si detector for low-energy X-rays.

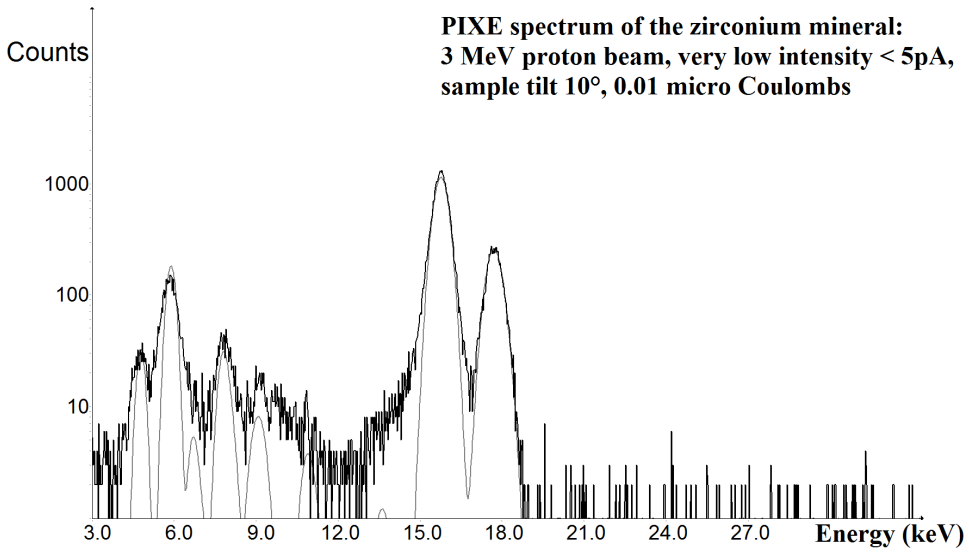

Fig. 18: PIXE spectrum of zirconium mineral. The PIXE conditions as described in the figure. The GUPIXWIN output with data and fit is displayed. Zirconium Kα lines are well visible together with escape peaks. Small amount of Hf can be visible as well (L-lines at 7.9, 9.0 and 10.5 keV). Problematic is overlapping with Zr escape peaks. Possible Ti presence in 4.5 – 4.9 keV region, but more probable is it a Zr escape peak. Presence of U is very plausible. GUPIXWIN found its Lα line at 13.6 keV, but it lies in the "tail" of Zr Kα line. The other uranium L lines lie in the Zr K lines, region; 15.7 – 17.7 keV.

PIGE measurements

Although the beam line is equipped with PIXE/PIGE detector, because of the absence of the radiation shield around the PIXE/PIGE chamber against neutrons, detail PIGE investigations have not been carried out yet, just very preliminary estimations. It is planned that all of the beam lines after the switching magnet will be shifted to the bunker so reactions with production of neutrons could be carried out as well.

First PIGE spectrum was measured from Teflon tape, which is rich on fluorine (Teflon – PTFE). The 3 MeV proton beam was used for this measurement, spectrum is displayed in Fig. 19. Protons were non-elastically scattered on the fluorine nuclei what can be seen from visible lines at 110, 197, 1236 and 1349 keV. Reactions with protons took place ^{19}F (p, p'γ), as described in [Kiss, 1985]. Possibly other materials with suitable proton reactions will be analyzed in the near future.

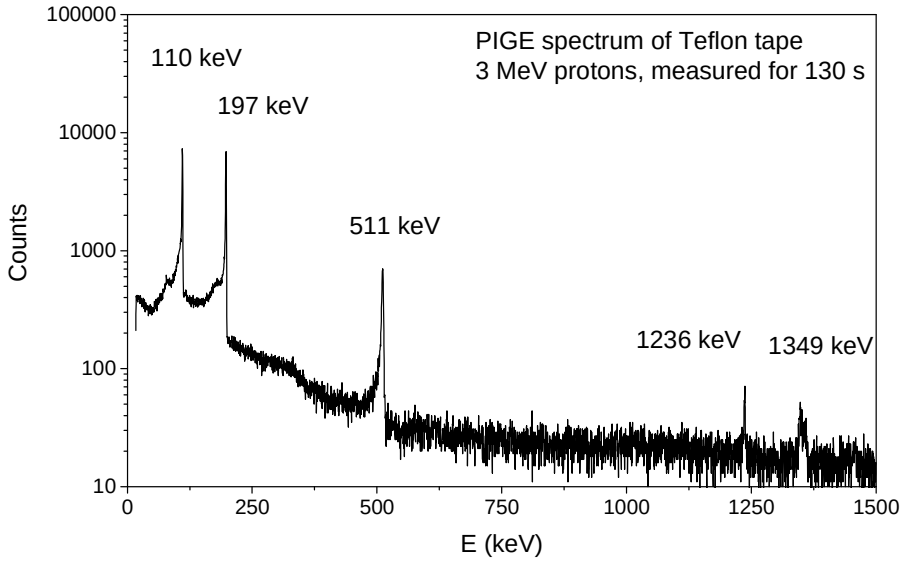

Fig. 19: PIGE spectrum of Teflon (PTFE) tape. Detected gamma lines with energies 110, 197, 1236 and 1349 keV indicate ^{19}F (p, p'γ) reactions. 511 keV annihilation line was detected as well. PIGE analyzes have not been performed yet, only some spectra were measured in order to test the detector for possible further PIGE analyzes.

Summary

The main results achieved in this thesis can be summarized as follows:

Transmission efficiencies for ^{1}H, ^{4}He, ^{9}Be and ^{12}C ions were determined for different values of terminal voltage, and their dependence on the stripper gas pressure was observed. Individual ions exhibit different behavior, depending on the charge state, terminal voltage and nitrogen pressure (the stripping gas). A common feature of all dependencies is a successive increase of the transmission efficiency with increasing stripper gas pressure to a certain point followed by a decrease of the transmission efficiency towards higher stripper gas pressures. This decrease is stronger for lower charge states ($^{4}He^{1+}$, $^{9}Be^{1+}$ and $^{12}C^{2+}$). Towards to higher charge states this decrease is less evident and becomes more flat (charge states $^{4}He^{2+}$, $^{9}Be^{2+}$ and even more for $^{9}Be^{3+}$ and for $^{12}C^{4+}$). The reason for such behavior is that with increasing the stripper gas pressure, both the electron stripping (which affects the transmission efficiency) and the ion scattering on molecules of the stripper gas are rising. Each ion has a combination of charge state, energy (guided by the terminal voltage of the tandem accelerator) and a certain value of stripper gas pressure at which the scattering process starts to reduce the final transmission efficiency. The smooth decrease of transmission efficiency for higher charge can be used for better stability of ion beams at these regions of stripper gas pressure for various applications, e.g. for ion irradiation or for applications of IBA techniques, which require stable ion beams. Working in these stable regions, the transmission efficiency is not affected by slight changes in the stripper gas pressure.

Simulations of $^{4}He^{2+}$ ion beam transversal profile were performed using SIMION software. The beam trajectories through the magnetic quadrupole triplet lens (QP) and the switching magnet (SM) were simulated. The final beam profile was monitored at the target distance (~2 m from the SM exit) in 45° channel. Models of these devices were created using the 3DCAD software Autodesk Inventor. Such models were placed into SIMION's workbench and the ions were flown through the system. The initial beam profile was circular with Gaussian distribution (5×5 mm FWHM), and the beam trajectory was in the axis of the beam line. Magnetic field of SM was simulated so the beam hit the center of target foil. For 3.052 MeV $^{4}He^{2+}$ ion beam the SM's magnetic field flux density was 3914.7 Gauss. Different setting of QP was simulated in order to obtain focused beam at the target distance. Various settings of QP exhibited both focusing as well as defocusing effects on the beam profile.

Finally, proper setting of QP was found and focused $^{4}He^{2+}$ ion beam with 1.4 mm diameter was simulated.

The PIXE chamber was installed in September 2015. Firstly, the BEGe detector was calibrated using point radioactive sources covering the energy spectrum of the detector. Three different settings of MCA's amplifier were calibrated; for low energies (up to ~ 60 keV), for medium energies (up to 500 keV) and for high energies (up to 3 MeV). Only results for low energies are stated in this work because the other are not important for purposes of PIXE measurements performed in the laboratory (they will be used for PIGE analyzes). First PIXE analyzes were performed on Slovak coins and laboratory PIXE standards consisting of pressed clean metallic powders (Ti, Fe, Cu, Zn and Ag) [Zeman, 2016B]. Each metallic powder mixture was prepared using a pneumatic press to form flat, coin-like, pellets. These analyzes had mostly qualitative character; we were able to observe a presence of elements in the samples and estimate the possible concentration comparing with the pressed powders standard samples. As we have found out later, the composition of such prepared mixtures is not uniform. We performed multiple PIXE measurements on different spots of each mixed powder sample and observed different relative concentrations of elements present in one sample depending on the measured spot. Therefore, for thick samples, another pressed powders samples were created using only single element powder to form pressed pellets. Nevertheless, the very first PIXE analyzes of Slovak coins taught us how to interpret the measured PIXE spectra and also how important is the knowledge of detector specifications.

For further fully quantitative PIXE analyzes, some adjustments in PIXE chamber had to be done. At first, in Slovak coins analyzed we observed high bremsstrahlung background. Therefore the BEGe detector was shifted into larger distance from the interaction point (center of the PIXE chamber). The new distance from this center increased from original 2.5 cm to 25 cm with impact on the background suppression. This distance was chosen for further analyzes, and is used currently (April 2017), as well. Next, additional electrode was installed into the PIXE chamber. Its purpose is to suppress the secondary emission of electrons after ion impact on the sample surface. This is important for quantitative PIXE analyzes due to proper charge collection process. SIMION simulations were used to find the proper dimensions of this electrode. The final shape and dimensions had to be suitable into the inside of the chamber and satisfy the SIMION simulations as well.

Quantitative PIXE analyzes require knowledge of the precise detector efficiency in order to retrieve information about absolute concentrations of element constituting monitored samples. For this purpose, BEGe detector efficiency was both measured and modelled.

Results are shown in Fig. 10. The modelled efficiency below 5 keV drops below a reasonable value. Therefore, quantitative analyzes of X–rays below 5 keV is complicated. This means that direct quantitative PIXE analysis can be performed starting with vanadium for K lines (4.952 keV) and praseodymium for L lines (5.033 keV). However, employing special strategies in sample treatment and spectra evaluation can reach lower X–ray energies, and even the detector efficiency can be "bypassed" using well-defined standard samples.

For direct quantitative analyzes a knowledge of H value is crucial together with detector efficiency. Depending on the detection system characterization, the energy dependency of H value can be observed. In well-defined system, the H value should be constant, independent on the X–ray energy. Any missing parameter or misinterpreted parameter can lead to dependency on the energy. In CENTA laboratory, H values for thin and thick targets were determined separately. Individual values were determined using pure elemental standards. Both, proton and helium beams were monitored and final H values for individual X–ray energies were determined using GUPIXWIN software. For thin samples, H value for protons exhibits energy dependency, but H value for helium beam is more-less constant. For thick samples, only H values for protons were determined because of technical issues (difficulties with Alphatross ion source). These H values exhibit energy dependency similar to thin samples measurements. Determined H values can be used for further PIXE analysis of different materials.

A special sample of rat brain slice was analyzed using the PIXE technique. This sample forms a special layered system of material which could have been analyzed by GUPIXWIN. The 3 MeV proton beam with 1.5 mm diameter was utilized for this analysis. The rat brain slice mounted on a silicon wafer and covered by thin gold film was placed into the PIXE chamber, and thin proton beam PIXE analyzes were performed on 12 different spots across the sample surface. The goal was to determine the iron concentration in this sample. GUPIXWIN was used for all analyzes and the final concentrations of iron in rat brain slice were determined on monitored positions with values up to 50 ppm, showing a clear gradient of concentrations.

Achieved results concerning development and utilization of IBA techniques show the range of taken effort to obtain reliable conclusions. Only 4 years before the laboratory hall was built (February 2013), then it was equipped with tandem accelerator and other units, and recently, PIXE measurements begun. The fact, that an iron concentration in a biological sample was determined reveals potential use of this technique, and next steps are directed to nuclear microprobe utilization.

References

[Alph, 2011] National Electrostatics Corp., Instruction manual No. 2JT002110 for RF Charge Exchange Ion Source. Middleton, 2011.

[Bend, 2011] National Electrostatics Corp., Instruction manual No. 2BA020240 for Analyzing magnet injection beamline. Middleton, 2011.

[Borysiuk, 2014] Borysiuk M. et al., Evaluation of a setup for pNRA at LIBAF for applications in geosciences, Nuclear Instruments and Methods in Physics Research B, vol. 332, p. 202–206, Elsevier, 2014.

[BPM, 2011] National Electrostatics Corp., Instruction Manual No. 2ET908110 for Operation and Service of Beam profile monitor model BPM81 (Integral collector). Middleton, 2011.

[Bykov, 2012] Bykov I. et al., Investigation of tritium analysis methods for ion microbeam application, Nuclear Instruments and Methods in Physics Research B, vol. 273, p. 251. Elsevier, 2012.

[Calligaro, 2001] Calligaro T. et al., ERDA with an external helium ion micro beam: Advantages and potential applications, Nuclear Instruments and Methods in Physics Research B, vol. 181, p. 180, Elsevier, 2001.

[Campbell, 2000] Campbell J.L., Hopman T.L., Maxwell J.A., Nejedly Z., The Guelph PIXE software package III: Alternative proton database, Nuclear Instruments and Methods in Physics Research B, vol. 170, p. 193 – 204. Elsevier, 2000.

[Campbell, 2010] Campbell J.L., Boyd N.I., Grassi N., Bonnick P., Maxwell J.A., The Guelph PIXE software package IV, Nuclear Instruments and Methods in Physics Research B, vol. 268, p. 3356–3363. Elsevier, 2010.

[Carella, 2014] Nuclear reaction analysis as a tool for the ^{3}He thermal evolution in Li_2TiO_3 ceramics, Nuclear Instruments and Methods in Physics Research B, vol. 332, p. 85–89, Elsevier, 2014.

[Calzolai, 2015] Calzolai G. et al., Improvements in PIXE analysis of hourly particulate matter samples, Nuclear Instruments and Methods in Physics Research B, vol. 363, p. 99–104, Elsevier, 2015.

[Chêne, 2012] Chêne G. et al., New external beam and particle detection set-up of Liège cyclotron – First applications of high energy beams to cultural heritage, Nuclear Instruments and Methods in Physics Research B, vol. 273, p. 209. Elsevier, 2012.

[Chu, 1978] Chu W.-K., Mayer J. W., Nicolet M.-A., Backscattering spectrometry, Academic Press, Inc., San Diego, 1978.

[Dapor, 2016] Dapor M., Abril I., de Vera P., Garcia-Molina R., Energy Deposited by Secondary Electrons Generated by Swift Proton Beams through Polymethylmethacrylate, International Journal of Chemical, Molecular, Nuclear, Materials and Metallurgical Engineering, vol. 10 (8), p. 992. World Academy of Science, Engineering and Technology, 2016.

[Denker, 2005] Denker A. et al., High-energy PIXE using very energetic protons: quantitative analysis and cross-sections, X-Ray Spectrom., vol. 34, p. 376–380, Wiley, 2005.

[EL1, 2017] online: http://en.wikipedia.org/wiki/Einzel_lens

[EL2, 2011] National Electrostatics Corp., Instruction Manual No. 2ET067180 for Operation and Service of EINZEL LENS Model EL76-60. Middleton, 2011.

[ERDA, 2016] online: http://www.spirit-ion.eu/v1/Project/Techniques/ERDA.html

[ESA, 2011] National Electrostatics Corp., Instruction manual No. 2EA071000 for ESA, INJECTOR. Middleton, 2011.

[ESXY, 2011] National Electrostatics Corp., Instruction Manual No. 2ET903100 for Operation of Electrostatic steerers. Middleton, 2011.

[FC50, 2011] National Electrostatics Corp., Instruction manual No. 2ET952300 for Faraday cup model no. FC50. Middleton, 2011.

[Guillou, 2014] Thermal behavior of deuterium implanted into nuclear graphite studied by NRA, Nuclear Instruments and Methods in Physics Research B, vol. 332, p. 90–94, Elsevier, 2014.

[Kaplan, 2016] Kaplan S. et al., Electromagnetic field and brain development, Journal of Chemical Neuroanatomy, vol. 75, p. 52–61. Elsevier, 2016.

[Karydas, 2014] Karydas A. G. et al., In-depth elemental characterization of Cu(In,Ga)Se_2 thin film solar cells by means of RBS and PIXE techniques, Nuclear Instruments and Methods in Physics Research B, vol. 331, p. 93–95, Elsevier, 2014.

[Kiss, 1985] Kiss Á. Z. et al., Measurements of relative thick target yields for PIGE analysis on light element in the proton energy interval 2.4 – 4.2 MeV, J Radioanal Nucl Chem, vol. 89, p. 123-141. Springer, 1985.

[Kostoff, 2013] Kostoff R.N., Lau G.Y.C., Combined biological and health effects of electromagnetic fields and other agents in the published literature, Technological Forecasting & Social Change, vol. 80, p. 1331–1349. Elsevier, 2013.

[NPL, 2017] available online at National Physical laboratory webpage: http://www.kayelaby.npl.co.uk/atomic_and_nuclear_physics/4_2/4_2_1.html

[Magalhães, 2012] Magalhães S. et al., High precision determination of the InN content of $Al_{1-\chi}$ $In_\chi N$ thin films by Rutherford backscattering spectrometry, Nuclear Instruments and Methods in Physics Research B, vol. 273, p. 105. Elsevier, 2012.

[Manuel, 2014] Manuel J.E. et al., Fish gelatin thin film standards for biological application of PIXE, Nuclear Instruments and Methods in Physics Research B, vol. 332, p. 37–41, Elsevier, 2014.

[Martin, 2012] Martin G. et al., Irradiation damage effects on helium migration in sintered uranium dioxide, Nuclear Instruments and Methods in Physics Research B, vol. 273, p. 123. Elsevier, 2012.

[Martin, 2003] Martin J. W. et al., The Local Chemical Analysis of Materials, Pergamon Materials Series, vol. 9, p. 112. Elsevier, 2003.

[Mathayan, 2016] Mathayan V., Balakrishnan S., Panigrahi B., Lattice location of O^{18} in ion implanted Fe crystals by Rutherford backscattering spectrometry, channeling and nuclear reaction analysis, Nuclear Instruments and Methods in Physics Research B, vol. 383, p. 47–51, Elsevier, 2016.

[Maxeiner, 2015] Maxeiner S. et al., Simulation of ion beam scattering in a gas stripper, Nuclear Instruments and Methods in Physics Research B, vol. 361, p. 242, Elsevier, 2015.

[Maxwell, 1989] Maxwell J.A., Campbell J.L., Teesdale W.J., The Guelph PIXE software package, Nuclear Instruments and Methods in Physics Research B, vol. 42, p. 218 – 230. Elsevier, 1989.

[Maxwell, 1995] Maxwell J.A., Teesdale W.J., Campbell J.L., The Guelph PIXE software package II, Nuclear Instruments and Methods in Physics Research B, vol. 95, p. 407 – 421. Elsevier, 1995.

[Mayer, 2012] Mayer M. et al., Rutherford backscattering analysis of porous thin TiO2 films, Nuclear Instruments and Methods in Physics Research B, vol. 273, p. 83. Elsevier, 2012.

[MicroM, 2017] webpage of the company: http://www.micromatter.com/xrf.php

[Morilla, 2012] Morilla Y. et al., Developing the IBA equipment to increase the versatility of the CNA, Nuclear Instruments and Methods in Physics Research B, vol. 273, p. 221. Elsevier, 2012.

[Msimanga, 2012] Msimanga M. et al., Heavy ion energy loss straggling data from Time of Flight stopping force measurements, Nuclear Instruments and Methods in Physics Research B, vol. 273, p. 6. Elsevier, 2012.

[MS-Y, 2011] MS-Y] National Electrostatics Corp., Instruction manual No. 2EA032940 for Magnetic Steerer. Middleton, 2011.

[Nakai, 2015] Nakai K. et al., Boron analysis for neutron capture therapy using particle-induced gamma-ray emission, Applied Radiation and Isotopes, vol. 106, p. 166–170, Elsevier, 2015.

[Nastasi, 2015] Nastasi M., Mayer J.W., Wang Y., Ion beam analysis: fundamentals and applications. CRC Press, Boca Raton, 2015.

[NRA, 2016] online: http://www.spirit-ion.eu/v1/Project/Techniques/NRA.html

[Ortega, 2010] Ortega-Feliu I. et al., A comparative study of PIXE and XRF corrected by Gamma-Ray Transmission for the non-destructive characterization of a gilded roman railing, Nuclear Instruments and Methods in Physics Research B, vol. 268, p. 1920–1923, Elsevier, 2010.

[Paneta, 2014] Paneta V. et al., Study of the ^{24}Mg (d, $p_{0, 1, 2}$) reactions at energies and angles relevant to NRA, Nuclear Instruments and Methods in Physics Research B, vol. 319, p. 34–38, Elsevier, 2014.

[Patronis, 2014] Patronis N. et al., Study of $^{nat}Mg(d,d_0)$ reaction at detector angles between 90° and 170°, for the energy range $E_{d,lab}$=1660–1990 keV, Nuclear Instruments and Methods in Physics Research B, vol. 337, p. 97–101, Elsevier, 2014.

[Pellegrino, 2012] Pellegrino S. et al., The JANNUS Saclay facility: A new platform for materials irradiation, implantation and ion beam analysis, Nuclear Instruments and Methods in Physics Research B, vol. 273, p. 216. Elsevier, 2012.

[Pelletron1, 2017] online: http://www.pelletron.com/tutor.htm

[Pelletron2, 2017] online: http://www.pelletron.com/negion.htm

[Pelletron3, 2017] online: http://www.pelletron.com/charging.htm

[Petersson, 2012] Petersson P. et al., Nuclear reaction and heavy ion ERD analysis of wall materials from controlled fusion devices: Deuterium and nitrogen-15 studies, Nuclear Instruments and Methods in Physics Research B, vol. 273, p. 113. Elsevier, 2012.

[Pichon, 2010] Pichon L., Beck L., Walter Ph., Moignard B., Guillou T., A new mapping acquisition and processing system for simultaneous PIXE-RBS analysis with external beam, Nuclear Instruments and Methods in Physics Research B, vol. 268, p. 2028–2033, Elsevier, 2010.

[Povinec, 2015] Povinec P. et al., A new IBA-AMS laboratory at the Comenius University in Bratislava (Slovakia), Nuclear Instruments and Methods in Physics Research B, vol. 342, p. 324. Elsevier, 2015.

[Povinec, 2015B] Povinec P. et al., Development of the Accelerator Mass Spectrometry technology at the Comenius University in Bratislava, Nuclear Instruments and Methods in Physics Research B, vol. 361, p. 88. Elsevier, 2015.

[Povinec, 2016] Povinec P.P., Masarik J., Ješkovský M., Breier R., Kaizer J., Pánik J., Richtáriková M., Staníček J., Šivo A., Zeman J., Recent results from the AMS/IBA laboratory at the Comenius University in Bratislava: preparation of targets and optimization of ion sources, J Radioanal Nucl Chem, vol 307, p. 2101–2108. Springer, 2016.

[Reiche, 2006] Reiche I. et al., Analyses of hydrogen in quartz and in sapphire using depth profiling by ERDA at atmospheric pressure: Comparison with resonant NRA and SIMS, Nuclear Instruments and Methods in Physics Research B, vol. 249, p. 609. Elsevier, 2006.

[Sério, 2012] Sério S. et al., Incorporation of N in TiO2 films grown by DC-reactive magnetron sputtering, Nuclear Instruments and Methods in Physics Research B, vol. 273, p. 110. Elsevier, 2012.

[SIMION, 2017] SIMION 8.0 user manual, chapter 2 – SIMION Basics, available online: http://simion.com/manual/chap2.html

[Steier, 2000] Steier P., Exploring the limits of VERA: A universal facility for accelerator mass spectrometry, dissertation, p. 57-64, Institut für Isotopenforchung und Kernphysik, VERA Labor, Vienna, 2000.

[Suárez, 2011] Moreno-Suárez A. I. et al., Combining non-destructive nuclear techniques to study Roman leaded copper coins from Ilipa (II–I centuries B.C.), Nuclear Instruments and Methods in Physics Research B, vol. 269, p. 3098–3101, Elsevier, 2011.

[Switch, 2011] National Electrostatics Corp., Instruction manual No. 2BA017470 for Switching magnet. Middleton, 2011.

[Terzi, 2016] Terzi M., Ozberk B., Deniz O.G., Kaplan S., The role of electromagnetic fields in neurological disorders, Journal of Chemical Neuroanatomy, vol. 75, p. 77–84. Elsevier, 2016.

[Tripathy, 2010] Tripathy B.B., Rautray T. R., Rautray A. C., Vijayan V., Elemental analysis of silver coins by PIXE technique, Applied Radiation and Isotopes, vol. 68, p. 454–458, Elsevier, 2010.

[Wiedemann, 2015] Wiedemann H., Particle accelerator physics, 4th edition, Graduate text in physics, p. 12, Springer, 2015.

[Winkler, 2015] Winkler S. R. et al., He stripping for AMS of 236U and other actinides using a 3 MV tandem accelerator, Nuclear Instruments and Methods in Physics Research B, vol. 361, p. 461, Elsevier, 2015.

[Založnik, 2016] Založnik A. et al., In situ hydrogen isotope detection by ion beam methods ERDA and NRA, Nuclear Instruments and Methods in Physics Research B, vol. 371, p. 167–173, Elsevier, 2016.

[Zeman, 2016] Zeman J., Ješkovský M., Pánik J., Staníček J., Povinec P.P., Pelletron transmission efficiency measurements for ^{9}Be and ^{12}C ions at the CENTA laboratory, Acta Physica Universitatis Comenianae, vol. 53, p. 95–100, Bratislava, 2016.

[Zeman, 2016B] Zeman J., Ješkovský M., Kaiser R., Kaizer J., Povinec P.P., Staníček J., PIXE beam line at the CENTA facility of the Comenius University in Bratislava: first results, J Radioanal Nucl Chem, vol. 309, DOI 10.1007/s10967-016-5004-1. Springer, 2016.

[Zucchiatti, 2015] Zucchiatti A. et al., Building a fingerprint database for modern art materials: PIXE analysis of commercial painting and drawing media, Nuclear Instruments and Methods in Physics Research B, vol. 363, p. 150–155, Elsevier, 2015.

UNIVERZITA KOMENSKÉHO
FAKULTA MATEMATIKY, FYZIKY A INFORMATIKY

Zoznam publikačnej činnosti

Mgr. Jakub Zeman

ADC Vedecké práce v zahraničných karentovaných časopisoch

ADC01 Povinec, Pavel P. [UKOMFKJFB] (10%) - Masarik, Jozef [UKOMFKJFB] (10%) - Ješkovský, Miroslav [UKOMFKJFB] (20%) - Kaizer, Jakub [UKOMFKJFB] (20%) - Šivo, Alexander [UKOMFKJFB] (5%) - Breier, Róbert [UKOMFKJFB] (5%) - Pánik, Ján [UKOMFKJFBd] (5%) - Staníček, Jaroslav [UKOMFKJFB] (5%) - Richtáriková, Marta [UKOMFKJFB] (5%) - Zahoran, Miroslav [UKOMFKEF] (10%) - Zeman, Jakub [UKOMFKJFBd] (5%): Development of the Accelerator Mass Spectrometry technology at the Comenius University in Bratislava
Lit. 50 zázn., 9 obr.
In: Nuclear Instruments and Methods in Physics Research Section B - Beam Interactions with Materials and Atoms. - Vol. 361 (2015), s. 87-94
Registrované v: wos, scopus

ADC02 Povinec, Pavel P. [UKOMFKJFB] (10%) - Masarik, Jozef [UKOMFKJFB] (10%) - Ješkovský, Miroslav [UKOMFKJFB] (10%) - Breier, Róbert [UKOMFKJFB] (10%) - Kaizer, Jakub [UKOMFKJFB] (10%) - Pánik, Ján [UKOMFKJFBd] (10%) - Richtáriková, Marta [UKOMFKJFB](10%) - Staníček, Jaroslav [UKOMFKJFB] (10%) - Šivo, Alexander [UKOMFKJFB] (10%) - Zeman, Jakub [UKOMFKJFBd] (10%): Recent results from the AMS/IBA laboratory at the Comenius University in Bratislava: preparation of targets and optimization of ion sources
Lit. 50 zázn.
In: Journal of Radioanalytical and Nuclear Chemistry. - Vol. 307, No. 3 (2016), s. 2101-2108
Registrované v: wos, scopus

ADC03 Zeman, Jakub [UKOMFKJFBd] (50%) - Ješkovský, Miroslav [UKOMFKJFB] (10%) - Kaiser, Ralf (10%) - Kaizer, Jakub [UKOMFKJFB] (10%) - Povinec, Pavel P. [UKOMFKJFB] (10%) - Staníček, Jaroslav [UKOMFKJFB] (10%): PIXE beam line at the CENTA facility of theComenius University in Bratislava: first results
Lit. 30 zázn., 5 obr., 2 tab.
In: Journal of Radioanalytical and Nuclear Chemistry. - Vol. 311, No. 2 (2017), s. 1409-1415
Registrované v: scopus

AED Vedecké práce v domácich recenzovaných vedeckých zborníkoch, monografiách

AED01 Pánik, Ján [UKOMFKJFBd] (20%) - Ješkovský, Miroslav [UKOMFKJFB] (20%) - Kaizer, Jakub [UKOMFKJFB] (20%) - Zeman, Jakub [UKOMFKJFBd] (20%) - Povinec, Pavel P. [UKOMFKJFB] (20%): Investigations of aluminium compounds as targets in the SNICS ionsource of the CENTA laboratory
Lit. 6 zázn., 14 obr., 5 tab.
In: Acta Physica Universitatis Comenianae-New Series, Vol. 53. - Bratislava : Comenius University Press, 2016. - S. 83-94. - ISBN 978-80-223-4197-4

AED02 Zeman, Jakub [UKOMFKJFBd] (20%) - Ješkovský, Miroslav [UKOMFKJFB] (20%) - Pánik, Ján [UKOMFKJFBd] (20%) - Staníček, Jaroslav [UKOMFKJFB] (20%) - Povinec, Pavel P. [UKOMFKJFB] (20%): Pelletron transmission efficiency measurements for 9Be and 12Cions at the CENTA laboratory
Lit. 8 zázn., 2 obr., 3 tab.
In: Acta Physica Universitatis Comenianae-New Series, Vol. 53. - Bratislava : Comenius University Press, 2016. - S. 95-100. - ISBN 978-80-223-4197-4

AFD Publikované príspevky na domácich vedeckých konferenciách

AFD01 Zeman, Jakub [UKOMFKJFBd] (100%) : Korekcie na efekty ovplyvňujúce koincidenčné merania 22Na

v aerosóloch atmosféry Bratislavy
Lit. 8 zázn., 12 obr.
In: Študentská vedecká konferencia FMFI UK, Bratislava 2013 : Zborník príspevkov. - Bratislava : Fakulta matematiky, fyziky a informatiky UK, 2013. - S. 59-63. - ISBN 978-80-8147-009-7
[Študentská vedecká konferencia FMFI UK 2013. Bratislava, 23.4.2013]

AFG Abstrakty príspevkov zo zahraničných vedeckých konferencií

AFG01 Povinec, Pavel P. [UKOMFKJFB] (10%) - Masarik, Jozef [UKOMFKJFB] (10%) - Holý, Karol [UKOMFKJFB] (10%) - Ješkovský, Miroslav [UKOMFKJFB] (10%) - Breier, Róbert [UKOMFKJFB] (10%) - Šivo, Alexander [UKOMFKJFB] (10%) - Staníček, Jaroslav [UKOMFKJFB](10%) - Kaizer, Jakub [UKOMFKJFB] (10%) - Pánik, Ján [UKOMFKJFBd] (10%) - Zeman, Jakub [UKOMFKJFBd] (10%): A new AMS laboratory at the Comenius University in Bratislava
In: AMS-13 The Thirteenth International Conference on Accelerator Mass Spectrometry : Programme and Abstracts Handbooks. - Marseille : Aix - Marseille University, 2014. - S. 27
[AMS 2014 : Accelerator Mass Spectrometry : International Conference. 13th, Aix en Provence, 24.-29.8.2014]

AFH Abstrakty príspevkov z domácich vedeckých konferencií

AFH01 Pánik, Ján [UKOMFKJFBd] (15%) - Ješkovský, Miroslav [UKOMFKJFB] (15%) - Kaizer, Jakub [UKOMFKJFB] (15%) - Povinec, Pavel P. [UKOMFKJFB] (15%) - Richtáriková, Marta [UKOMFKJFB] (15%) - Šivo, Alexander [UKOMFKJFB] (15%) - Zeman, Jakub [UKOMFKJFBd](10%): Development of methods for assessment of radionuclides around nuclear power plants using accelerator mass spectrometry
In: 36th Days of Radiation Protection : Book of Abstracts. - Bratislava : Slovak Medical University, 2014. - S. 96. - ISBN 978-80-89384-08-2
[Days of Radiation Protection 2014. 36th, Poprad, 10.-14.11.2014]

BFA Abstrakty odborných prác zo zahraničných podujatí (konferencie, ...)

BFA01 Povinec, Pavel P. [UKOMFKJFB] (9%) - Masarik, Jozef [UKOMFKJFB] (9%) - Ješkovský, Miroslav [UKOMFKJFB] (9%) - Breier, Róbert [UKOMFKJFB] (9%) - Kaizer, Jakub [UKOMFKJFB] (9%) - Kováčik, Andrej [UKOMFKJFBs] (8%) - Pánik, Ján [UKOMFKJFBd] (9%) - Richtáriková, Marta [UKOMFKJFB] (9%) - Šivo, Alexander [UKOMFKJFB] (9%) - Staníček, Jaroslav [UKOMFKJFB] (9%) - Zeman, Jakub [UKOMFKJFBd] (9%) - Steier, Peter (1%) - Priller, Alfred (1%): Accelerator mass spectrometry laboratory at the Comenius Universityin Bratislava: first results
Lit. 4 zázn., 1 obr.
In: ENVIRA 2015 : International Conference : Environmental Radioactivity [elektronický zdroj]. - Thessaloniki : Aristotle University, 2015. - nestr. [1 s.] [USB kľúč]
[ENVIRA 2015 : Environmental Radioactivity : International Conference. Thessaloniki, 21.-25.9.2015]

Štatistika kategórií (Záznamov spolu: 9):
ADC Vedecké práce v zahraničných karentovaných časopisoch (3)
AED Vedecké práce v domácich recenzovaných vedeckých zborníkoch, monografiách (2)
AFD Publikované príspevky na domácich vedeckých konferenciách (1)
AFG Abstrakty príspevkov zo zahraničných vedeckých konferencií (1)
AFH Abstrakty príspevkov z domácich vedeckých konferencií (1)
BFA Abstrakty odborných prác zo zahraničných podujatí (konferencie, ...) (1)

28.4.2017